Articles

Design and Theoretical Study of Nickel Catalysts for Syndiotactic Polyolefins

LIU, Ying*,[a](刘颖) LIU, Yue[a](刘跃) DREW, G. B. Michael[b] LIU, Jia-Wen[a](刘佳雯)

[a] *Department of Chemistry, Harbin Normal University, Harbin, Heilongjiang 150080, China*

[b] *Department of Chemistry, Reading University, Whiteknights, Reading RG6 6AD, U. K.*

A nickel catalyst was modeled with ligand L^2, [NH = CH—CH = CH—O]$^-$, which should have potential use as a syndiotactic polyolefin catalyst, and the reaction mechanism was studied by theoretical calculations using the density functional method at the B3LYP/LANL2MB level. The mechanism involves the formation of the intermediate [NiL^2Me]$^+$, in which the metal occupies a T-shaped geometry. This intermediate has two possible structures with the methyl group *trans* either to the oxygen or to the nitrogen atom of L^2. The results show that both structures can lead to the desired product via similar reaction paths, A and B. Thus, the polymerization could be considered as taking place either with the alkyl group occupying the position *trans* to the Ni—O or *trans* to the Ni—N bond in the catalyst. The polymerization process thus favors the catalysis of syndiotactic polyolefins. The syndiotactic synthesis effects could also be enhanced by variations in the ligand substituents. From energy considerations, we can conclude that it is more favorable for the methyl group to occupy the *trans*-O position to form a complex than to occupy the *trans*-N position. From bond length considerations, it is also more favoured for ethene to occupy the *trans*-O position than to occupy the *trans*-N position.

Keywords nickel catalyst, density functional method, polyolefin, mechanism

Introduction

Polyethylene (PE) is a very important industrial material. The discovery of polyethylene catalysts by Ziegler and Natta produced great advantages to the polyethylene industry. The mode and mechanism of action of these systems still remain a topic of current research. Following Ziegler-Natta catalysts, a new series of single active center polyolefin catalysts were discovered,[1] most of which were based on early transition metal d^0 complexes, and these are now extensively used for the polymerization of non-polar olefins such as ethene and propene. However, due to their highly oxophilic nature, these catalysts are incompatible with functionalized vinyl monomers. Moreover, these sensitive systems require "air-free" handling and rigorous exclusion of moisture. Yet despite these difficulties, the formation of such cationic metal centers remains the single most common design feature for polymerization catalysts.[2] Late transition metals are characteristically less oxophilic than the early transition metals and are thus more tolerant to functional groups, so the development of polyolefin catalysts has been concentrated on novel late transition metal complexes.[3] Variations in the structure of the catalysts have been used to produce a variety of polymers with novel uses and properties. Thus, for example, in 1995, Brookhart *et al.*[4] reported a nickel complex containing a diimine ligand L^1[L: ArN = C(R)C(R) = NAr; Ar: 2,6-C_6H_3(*i*-Pr)$_2$ and 2,6-$C_6H_3Me_2$; R: H and Me] which produced a branched polyethylene in the absence of co-monomers with considerable activity for ethylene polymerization. Subsequently in 1996, Brookhart *et al.*[5,6] established ethylene/methyl acrylate copolymerization using the corresponding palladium complex with L^1. Many attempts have been made to control the formation of polymer microstructures. Ligands play the most important role in the polymerization process, so varying the ligand can lead to variations in the products obtained. In this study, we focused on non-symmetric ligands because transition metal complexes bearing asymmetric ligands have been investigated less often than symmetric olefin polymerization catalysts.[7] Nickel diimine catalysts have been shown to preferentially produce isotactic polyolefins. So by replacing a nitrogen atom with an oxygen atom in the ligand, it might well favour the synthesis of syndiotactic polyolefins. Stereoselective catalysis will necessarily require asymmetric catalysts and this has been confirmed experimentally.[3] We chose salicylaldimine as the scaffold, because this ligand system allowed manipulation of both the steric and electronic parameters of the metal center.[3] Based on this concept, we modeled a nickel catalyst with L^2 ([NH = CH—CH = CH—O]$^-$), and report here the theoretical results.

Computational details

Geometries and energies of the species involved are calculated by using the gradient-corrected density functional theory B3LYP[8] implemented in the Gaussian 98 program.[9-13] The method has been shown to be quite reliable both in geometry

* E-mail: yuesd@0451.com

Received August 20, 2002; revised November 6, 2002; accepted January 14, 2003.

Project supported by the Natural Science Foundation of Heilongjiang Educational Committee of China (Nos. 10531081 and 10511033).

and in energy for these types of transition metal complexes.[14] In these calculations we used the LANL2MB basis set, because it has been shown[15] that larger basis sets did not change the results significantly for the model system. The modeled reaction mechanism is shown in Scheme 1.

The mechanism can be summarized as the following. Once activation has occurred after **1**, chain initialization proceeds via perpendicular uptake of an ethene into the free site of the square-planar metal center, so that a π-complex **2** is formed, and then the ethylene rotates into the plane **3** so that an insertion reaction can occur. After this insertion reaction of **4**, a β-agostic hydrogen bond in **5** is formed between Ni and β-C so as to assist the formation of a new vacant site and to realize chain propagation.

There are two possible structures for the starting cation species in the mechanism, with the methyl group occupying either a position *trans* to the oxygen atom (Path A) or the nitrogen atom (Path B) of L^2. As expected, there are subtle structure differences between the corresponding species in the two path. Given the specific starting structure, the reaction can proceed along similar pathways. The purpose of the calculation is to show that both the pathways are possible, which is the necessary condition to make the syndiotactic synthesis feasible via a process for an alkyl group to occupy alternatively at a position *trans* to the nitrogen atom and to the oxygen atom of L^2. The other purpose of the calculation is to investigate the structural and energetic differences in the two paths, which will provide useful information for future syndiotactic synthesis.

Results and discussion

As suggested by Brookhart,[4] we[16] have assumed the active catalyst initiating reaction to be the cation complex $[NiL^2CH_3]^+$ (**1A** or **1B**). The two paths proceed similarly, but with subtle differences in structures and energies. As shown in Scheme 1, the species **1A** or **1B** is calculated to be a minimum with a T-shaped planar (nearly C_s symmetry) structure. Among the bonds of Ni—N and Ni—O in **1A** or in **1B**, the bond which is *trans* to the methyl group has a longer length. The C(1)—H(1) bond in the methyl C_s plane is longer than the other two for both **1A** and **1B**, indicating a weak α-agostic interaction with the metal Ni. In both paths, the initial step of the reaction is the coordination of ethene to the reactant **1**. Two π-complexes were found with ethene either perpendicular or parallel respectively to the equatorial $[NiL^2Me]^+$ plane. Relative to the parallel complex **3**, the perpendicular **2** is lower in energy by 30.78 $kJ \cdot mol^{-1}$ for path B, presumably because of the larger steric repulsion. There is a similar result for path A.

The Ni—C(1), Ni—N, and Ni—O bond lengths in **2** are stretched relative to those found in the reactant **1**, indicating that an activation process is starting. The ethene is slightly activated as the bond length of C(2)—C(3) is stretched compared with the value of 0.1332 nm in free ethene. The binding energy of ethene for the π-complex **2** is −138.88 and −112.94 $kJ \cdot mol^{-1}$ for path A and path B respectively. Starting from **2**, insertion of the ethene into the Ni-methyl bond proceeds initially via rotation of the ethene moiety into the molecular plane, to give the structure **3**. The Ni—C(2) and the Ni—C(3) distances in **3** are longer than those observed for typical Ni—C σ-bonds.[17] The Ni—C(1), Ni—N, and Ni—O bond lengths in **3** are all stretched relative to the reactant **1**. The olefin maintains its activated state as its bond length in the complex **3** is still stretched. From **3**, the coordinated ethene then inserts into the Ni-methyl bond. The migratory insertion step results in the breaking of the Ni—C(1) bond and a Ni—C_2H_4 interaction, forming a new bond C(1)—C(2) and further reducing the Ni—C(3) bond length in **3**, and leading to the γ-agostic propyl complex **4**. The C(2)—C(3) bond length increases further in the γ-agostic product 4. The C(1)—H(2) and the C(1)—H(3)

Scheme 1 Mechanism of chain initialization of the Ni-catalyzed ethylene polymerization reaction

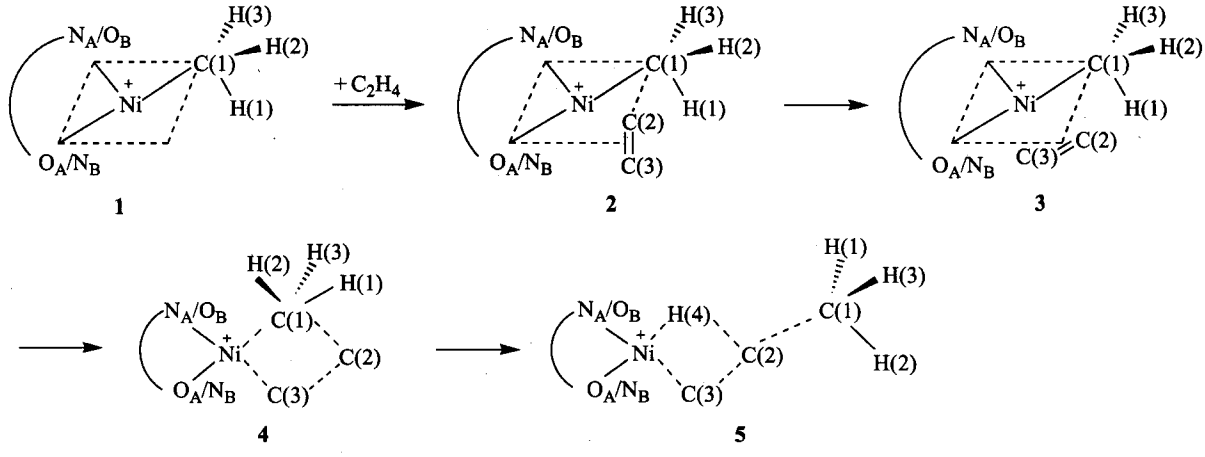

Following cocatalyst activation of a precatalyst, a methyl cation $[NiL^2Me]^+$ (**1**) is formed. The hydrogen atoms on C(2) and C(3) have been omitted for clarity. After **5** an ethylene molecule replaces H(4) to form a π-bond with nickel, the process is repeated.

bonds are involved in the γ-agostic interaction because both the two bond lengths are longer than the C(1)—H(1) bond length. In this γ-agostic complex **4**, one should notice a slightly longer C(1)—C(2) bond distance of 0.1568 nm compared with the normal CH_3—CH_2 distance of 0.1556 nm at the same level of theory, suggesting a β-agostic interaction with the C(1)—C(2) bond. It should be mentioned here that for path B, the alkyl group reverts to a position *trans* to the Ni—O bond, which is more favourable in energy. From the γ-agostic complex **4**, the ethyl group can be rotated around the C(2)—C(3) bond to form the β-agostic complex **5**. The β-agostic species is confirmed to be a real minimum and has only one β-agostic interaction. Due to the β-agostic interaction, the C(2)—H(4) bond in **5** is longer than the other C—H on C(2) in **5**. The Ni—H(4) distance is also very short and the Ni-C(3)-C(2) angle is well below the normal trigonal angle, indicating a very strong β-agostic interaction in **5**. The entire chain initiation reaction is exothermic.

From the above analysis, it is apparent that despite the difference in methyl position, the two pathways are similar and can lead to ethene polymerization. However some differences are apparent, thus the Ni—C(1) and the C(1)—H(1) bonds in the **1A** are shorter than those in **1B**. The net Mulliken charges on Ni for the various species in the mechanisms are shown in Table 1.

Table 1 Net charge (e) on the nickel atom in species **1**, **2**, **3**, **4**, **5** on paths A and B

	1	2	3	4	5
Ni (Path A)	0.352	0.193	0.184	0.291	0.269
Ni (Path B)	0.338	0.198	0.194	0.293	0.276

The energy of **1A** is 26.83 kJ·mol^{-1} lower than that of **1B**, thus suggesting that A is the most likely reaction path initiated from **1A**. The charge on Ni in **1A** is slightly greater by 0.014 e than in **1B**. The Ni—C (olefin) distances in **2A** are longer than those in **2B**, suggesting that ethene is more tightly bound when it lies in a position *trans* to the Ni—O bond. The charge on the metal in **2A** and **2B** is 0.193 and 0.198 e respectively. Because of the coordination of ethene, the charge on the nickel atom in both **2A** and **2B** is reduced by nearly half relative to **1**. Here, the charge on Ni in **2B** is slightly more than in **2A**, which supports the view that the coordination of ethene in **2B** is tighter than that in **2A**, due to better electron feedback from Ni to ethene in **2B**. The comparison of **3A** with **3B** is similar to that of **2A** with **2B**. The Ni—C(2) and the Ni—C(3) distances are 0.2545 and 0.2358 nm in **3A**, and 0.2414 and 0.2164 nm in **3B**, respectively. It is again indicative of tighter binding by the fact that the Ni—C (olefin) distances in **3B** are shorter than those in **3A**. Similarly the charge on Ni in **3B** is greater than that in **3A**. The parallel complex **3A** has an energy only 18.57 kJ·mol^{-1} below that of **3B** despite the fact that the difference between the energies of the perpendicular complexes is 25.94 kJ·mol^{-1}. From the above comparison, it can be concluded that the coordination of ethene to the *trans*-Ni—O is favoured. However, there is a striking change in the energy profile of paths A and B when the structures **4** and **5** are considered, in that both **4B** and **5B** have significantly lower energies than **4A** and **5A** respectively. The reason for this change is that the insertion of the coordinated ethene into the Ni—CH_3 bond leads to alkyl position exchange in the equatorial plane. The energy of **4B** is 25.25 kJ·mol^{-1} lower than that of **4A** and the Ni—C(3) and Ni—N bond lengths in **4B** are shorter than those in **4A**, unlike the observed trend for the corresponding bond lengths of Ni—C(1) and Ni—N in **1A** and **1B**, indicating the switching of the *trans* position to the alkyl group. The charge on Ni in **4B** is still slightly greater than in **4A**, also opposite to the observed trend in **1A** and **1B**. The energies of **5A** and **5B** follow a similar pattern with **5B** 15.99 kJ·mol^{-1} lower in energy than **5A**. The Ni—N bond length in **5B** (0.1850 nm) is shorter than that in **5A** (0.1959 nm) while the Ni—O bond lengths are 0.1947 nm, 0.1857 nm in **5B** and **5A** respectively. By comparing the relative energies of **1A** and **1B**, and then **4A** and **4B** with **5A** and **5B**, it can be concluded that the alkyl cation complex is more stable when the alkyl group lies in a position *trans* to the Ni—O bond.

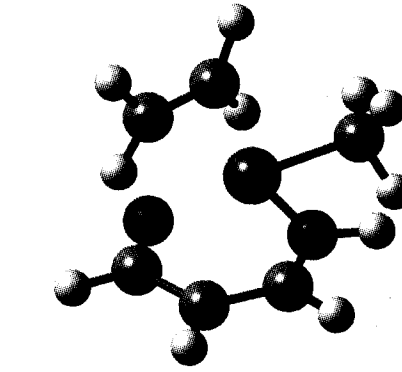

TS(2-3)A

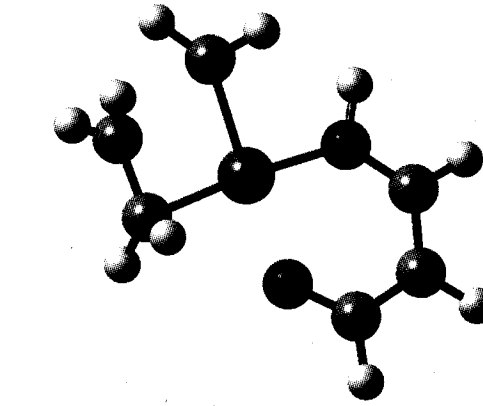

TS(3-4)A

Fig. 1 Optimized transition state geometries for path A between **2** and **3** [**TS(2-3)A**] and between **3** and **4** [**TS(3-4)A**].

The optimized transition state geometries for path A between **2** and **3** [**TS(2-3)A**] and between **3** and **4** [**TS(3-4)A**] are shown in Fig. 1. The energy and geometry of **TS(2-3)** are very close to those of **3**. The energy of **TS(2-3)B** for

path B is only 0.55 kJ·mol^{-1} higher than that of **3B**. It has only one imaginary frequency of 64.34*i* cm^{-1}, and the vector of this vibration corresponding mainly to the rotation of the ethene moiety in the catalyst. **TS(3-4)A** is confirmed to be the transition state of insertion reaction situated between **3** and **4**. It has only one imaginary frequency of 361.7*i* cm^{-1}. The activation energy from **3** is 17.60 kJ·mol^{-1}. The corresponding transition states for path B show similar behavior.

Conclusion

We have studied the polymerization of ethene with a nickel catalytic center coordinated to [HN=CH—CH=CH—O]$^-$. There are two possible structures with microstructure differences which could be enhanced by variation in ligand substituents for the active centre. The effects on the structure of the alkyl group are different depending on its position relative to the catalyst, thus providing potential use as a syndiotactic polyolefin catalyst. The syndiotactic polymerization can be explained from the two similar reaction paths. The most favourable structure is when the alkyl group occupies a position *trans* to the Ni—O bond. Ethene is more tightly bound to nickel when it coordinates to the *trans*-Ni—O position. If the preference was too strong, it would be act as a poison affecting the catalyst.

Chain initialization has been investigated and it can be concluded that both paths discussed above are feasible catalytic reaction mechanisms. The initiation reaction should start from **1A** according to energy considerations, as the alkyl cation complex is shown to be more stable when the alkyl group lies in a position *trans* to the Ni—O bond. The structure of the ethene complexes **2A** and **3A** are also more stable than **2B** and **3B**, where the ethene is added to **1A** *trans* to the Ni—N bond with the methyl group maintaining its position *trans* to the Ni—O bond, while the coordination of ethene to the *trans*-Ni—O position in **2B** or **3B** is tighter. The relative order of energies between paths A and B for compounds switches at complexes **4** and **5** and now the compounds in path B that the carbon atom of the alkyl group is *trans* to Ni—O becomes more stable.

Relative to alkyl cation complex **1**, the charge on Ni is decreased after the π-complex is formed in the two pathways respectively. After migratory insertion to give **4**, the charge on Ni is slightly reduced relative to the alkyl precursor **1**.

References

1 Huang, J.; Rempel, G. L. *Prog. Polym. Sci.* **1995**, *20*, 459.

2 Britovsek, G. J. P.; Gibson, V. C.; Wass, D. F. *Angew. Chem., Int. Ed.* **1999**, *38*, 428.

3 Younkin, T. R.; Connor, E. F.; Henderson, J. I.; Friedrich, S.; Li, R. T.; Grubbs, R. H.; Bansleben, D. A. *Science* **2000**, *287*, 460.

4 Johnson, L. K.; Killian, C. M.; Brookhart, M. *J. Am. Chem. Soc.* **1995**, *117*, 6414.

5 Johnson, L. K.; Mecking, S.; Brookhart, M. *J. Am. Chem. Soc.* **1996**, *118*, 267.

6 Killian, C. M.; Temple, D. J.; Johnson, L. K.; Brookhart, M. *J. Am. Chem. Soc.* **1996**, *118*, 11664.

7 Matsui, S.; Fujita, T. *Catal. Today* **2001**, *66*, 63.

8 (a) Becke, A. D. *Phys. Rev. A* **1988**, *38*, 3098.
(b) Lee, C.; Yang, W.; Parr, R. G. *Phys. Rev. B* **1988**, *37*, 785.
(c) Becke, A. D. *J. Chem. Phys.* **1993**, *98*, 5648.

9 Frisch, M. J.; Trucks, G. W.; Schlegel, H. B.; Scuseria, G. E.; Robb, M. A.; Cheeseman, J. R.; Zakrzewski, V. G.; Montgomery, J. A.; Jr, Stratmann, R. E.; Burant, J. C.; Dapprich, S.; Millam, J. M.; Daniels, A. D.; Kudin, K. N.; Strain, M. C.; Farkas, O.; Tomasi, J.; Barone, V.; Cossi, M.; Cammi, R.; Mennucci, B.; Pomelli, C.; Adamo, C.; Clifford, S.; Ochterski, J.; Petersson, G. A.; Ayala, P. Y.; Cui, Q.; Morokuma, K.; Rega, N.; Salvador, P.; Dannenberg, J. J.; Malick, D. K.; Rabuck, A. D.; Raghavachari, K.; Foresman, J. B.; Cioslowski, J.; Ortiz, J. V.; Baboul, A. G.; Stefanov, B. B.; Liu, G.; Liashenko, A.; Piskorz, P.; Komaromi, I.; Gomperts, R.; Martin, R. L.; Fox, D. J.; Keith, T.; Al-Laham, M. A.; Peng, C. Y.; Nanayakkara, A.; Challacombe, M.; Gill, P. M. W.; Johnson, B.; Chen, W.; Wong, M. W.; Andres, J. L.; Gonzalez, C.; Head-Gordon, M.; Replogle, E. S.; Pople, J. A. *Gaussian* 98, Revision A.11.2, Gaussian, Inc., Pittsburgh PA, **2001**.

10 Li, X.-Y.; Liu, J.-F.; Yu, H.-B. *Chin. J. Chem.* **2002**, *20*, 834.

11 Liu, Y; Wang, Q.; Su, Z.-M.; Liu, Y. *J. Mol. Sci.* **2002**, *18*, 98 (in Chinese).

12 Yang, X.-Z; Liu, Y.; Hsu, S. L. *Chin. J. Polym. Sci.* **1997**, *15*, 295.

13 Liu, Y.; Yang, X.-Z.; Dai, B.-Q.; Su, Z.-M.; Wang, Q. *Chem. Res. Chin. Univ.* **2001**, *17*, 315.

14 Musaev, D. G.; Morokuma, K. *J. Phys. Chem.* **1996**, *100*, 6509.

15 Musaev, D. G.; Svensson, M.; Morokuma, K.; Strömberg, S.; Zetterberg, K.; Siegbahn, P. E. M. *Organometallics* **1997**, *16*, 1933.

16 Liu, Y.; Liu, J.-W.; Yang, X.-Z. *Acta Phys.-Chim. Sinica* **2002**, *18*, 1068 (in Chinese).

17 Musaev, D. G.; Morokuma, K. *Adv. Chem. Phys.* **1996**, *96*, 61.

(E0208202 CHENG, B.; FAN, Y. Y.)